Phase-shift calibration algorithm for phase-shifting interferometry

Xin Chen, Maureen Gramaglia, and John A. Yeazell

Department of Physics, The Pennsylvania State University, University Park, Pennsylvania 16802

Received October 22, 1999; revised manuscript received March 31, 2000; accepted June 30, 2000

We propose a novel phase-shift calibration algorithm. With this technique we determine the unknown phase shift between two interferograms by examining the sums and differences of the intensities on each interferogram at the same spatial location, i.e., $I_1(x, y) \pm I_2(x, y)$. These intensities are normalized so that they become sinusoidal in form. A uniformly illuminated region of the interferograms that contains at least a 2π variation in phase is examined. The extrema of these sums and differences are found in this region and are used to find the unknown phase shift. An error analysis of the algorithm is provided. In addition, an error-correction algorithm is implemented. The method is tested by numerical simulation and implemented experimentally. The numerical tests, including digitization error, indicate that the phase step has a root-mean-square (RMS) phase error of less than 10^{-6} deg. Even in the presence of added intensity noise (5% amplitude) the RMS error does not exceed 1 deg. The accuracy of the technique is not sensitive to nonlinearity in the interferogram. [S0740-3232(00)01711-7]

OCIS codes: 120.2650, 120.3180.

1. INTRODUCTION

Phase-shifting interferometry provides phase information about an object beam by interfering it with a reference beam of known phase.[1,2] Standard techniques require a minimum of three interferograms with two controlled phase shifts to obtain the phase distribution, $\delta(x, y)$, of the object beam. The accuracy of these methods relies critically on the precision of these phase shifts.

A number of phase-calibration techniques have been developed to measure the phase shifts.[1–7] Perhaps the simplest technique[4] for phase-shifter calibration involves incrementing the phase delay of the reference beam until an interferogram identical to the initial interferogram is found. Clearly, the phase shift between these two interferograms is 2π. The intermediate phase shifts can be interpolated assuming that the phase shifting device behaves linearly. Nonlinear phase shifters and the search for an identical interferogram are the difficulties of this simple method. We will use this simple technique as a confirmation of the successful experimental implementation of the proposed calibration algorithm.

Many commonly used calibration techniques use variations of the Carré algorithm.[5] This algorithm records several interferograms for which the phase between any two consecutive images is shifted by an unknown but constant amount α. If four such interferograms are taken, the phase shift can be calculated by using the intensities at the same spatial location on all the interferograms. These methods assume that the phase shifter behaves linearly and that the only effect of incrementing the phase is that the phase is changed, e.g., there is no change in background intensity. These calibration techniques require some knowledge of the performance of the phase shifter (as above) or some knowledge of the phase structure of the interferogram. Also, fitting techniques have been developed that employ a series of interferograms.[6,7] The phase shifter is calibrated by fitting a function that depends on pairs of interferograms.

In this paper we present a phase calibration algorithm that does not require knowledge of the performance of the phase shifter. It also does not require the establishment of a special phase structure in the interferogram. All that is needed is that in some region of the interferogram the phase varies by at least 2π and that in that region the illumination is uniform. With these assumptions an arbitrary phase shift between two interferograms may be measured. As in Refs. 6 and 7, a function that depends on two interferograms is formed. However, no fitting is needed and no additional interferograms are necessary. A correlation technique that also uses only two interferograms has been proposed.[8] This technique works best if the region of interest contains precisely an integral number of fringes. If the number of fringes across the interferogram exceeds eight, the technique also yields excellent results. In this case, the accuracy of the phase step is 0.1% provided that the fringes are not too nonlinear. In this paper, we demonstrate a novel phase calibration algorithm that removes the need for such *a priori* knowledge of the phase shifter or of the nature of the interferogram (e.g., linearity). This calibration technique is also computationally efficient in that it scales linearly with the number of pixels of the interferogram. This calibration may be carried out *in situ* for each interferometric measurement. That is, it places only the above minor constraint on the phase characteristics of the object beam. This same insensitivity to the phase characteristics of the interferogram allows the phase-step measurement to be made to high accuracy even with rather ordinary optics.

2. PHASE-CALIBRATION ALGORITHM

The calibration algorithm may be visualized in terms of a Twyman–Green interferometer. The object beam has

the phase distribution $\delta(x, y)$. The phase of the reference beam is constant and may be shifted by a piezoelectric transducer (PZT). As in a typical interferometry experiment, the reference-beam phase is advanced and the resulting interferograms are recorded. In this calibration algorithm, an interferogram is recorded and then an arbitrary phase shift is applied to the reference beam, and a second interferogram is taken. We will assume that this phase shift ϕ is less than π. This simplifies the development by avoiding the problem of phase wrapping. A means of dealing with this phase-wrapping problem will be discussed in Section 5, where phase shifts of many π are measured in the experimental calibration of a phase shifter. The resulting two interferograms, before and after the phase shift are

$$I_1(x, y) = I_b(x, y) + I_m(x, y)\cos[\delta(x, y)], \tag{1}$$

$$I_2(x, y) = I_b(x, y) + I_m(x, y)\cos[\delta(x, y) + \phi], \tag{2}$$

where $I_b(x, y)$ is the background intensity and $I_m(x, y)$ is the modulation intensity. If the background intensity I_b and the modulation intensity I_m are constant over the region of interest, these interferograms may be reduced to simply cosine functions. This requirement on I_b and I_m is equivalent to requiring that different pixels in the region of interest are the same except for the effect of the phase term, $\delta(x, y)$. The region of interest is defined by the requirement that $\delta(x, y)$ vary by at least 2π or over a full fringe within this region so that the signal goes over both the maximum and the minimum. If such a region does not exist in a given phase distribution $\delta(x, y)$, then it can be created, e.g., by tilting one of the two mirrors to introduce the required 2π modulation.

In each interferogram, the maximum and minimum of the intensity may be found by examining the fringe in the region of interest. These extrema can be used to normalize the intensities so that the dependence of Eqs. (1) and (2) on I_b and I_m is eliminated. The normalized intensities are

$$I_{n1}(x, y) = \cos[\delta(x, y)], \tag{3}$$

$$I_{n2}(x, y) = \cos[\delta(x, y) + \phi]. \tag{4}$$

It should be noted that, even though in Eqs. (1) and (2) we have assumed that the two interferograms share the same I_b and I_m, the introduction of the normalization procedure allows a global change of background intensity between these two interferograms. Thus the normalization procedure makes the calibration algorithm insensitive to changes of the illuminating intensity (provided that the illumination remains spatially uniform). This effect may help to minimize the experimental error.

The normalized intensities are further used to find the phase shift, ϕ, between the two interferograms. The algorithm to find ϕ is based on the observation that the sum or difference of two cosine functions reveals the phase difference between them. Therefore we define Q_{12}^{+} as the sum of the normalized intensities of the two interferograms, $I_{n1}(x, y)$ and $I_{n2}(x, y)$:

$$Q_{12}^{+} = (1 + \cos\phi)\cos[\delta(x, y)] - \sin\phi\sin[\delta(x, y)]. \tag{5}$$

We define a variable R_{12}^{+} to be the difference between the maximum and the minimum of this sum Q_{12}^{+}. This range R_{12}^{+} is related to the phase shift ϕ by

$$R_{12}^{+} = \max[Q_{12}^{+}] - \min[Q_{12}^{+}] = 2\sqrt{2 + 2\cos\phi}. \tag{6}$$

Similarly, we define Q_{12}^{-} as the difference of the normalized intensities of the two interferograms $I_{n1}(x, y)$ and $I_{n2}(x, y)$:

$$Q_{12}^{-} = (1 - \cos\phi)\cos[\delta(x, y)] + \sin\phi\sin[\delta(x, y)]. \tag{7}$$

We define a range R_{12}^{-} to be the difference between the maximum and the minimum of Q_{12}^{-}. The relationship between R_{12}^{-} and the phase shift ϕ is

$$R_{12}^{-} = \max[Q_{12}^{-}] - \min[Q_{12}^{-}] = 2\sqrt{2 - 2\cos\phi}. \tag{8}$$

From R_{12}^{+} and R_{12}^{-} we can obtain the cosine of the phase shift,

$$\cos\phi = \frac{(R_{12}^{+})^2 - (R_{12}^{-})^2}{16}. \tag{9}$$

Thus the phase shift between the two interferograms has been isolated from $\delta(x, y)$, the position-dependent phase of the object beam. This equation is sufficient to determine ϕ. Equation (9) is the main result of this paper, as it allows the phase shift between two interferograms to be bound by using only the two interferograms themselves.

It should be noted that either the sum Q_{12}^{+} or the difference Q_{12}^{-} has sufficient information to retrieve the phase ϕ. However, the choice of a symmetric expression for the cosine term minimizes the error in the measurement. For example, with a limited number of samplings over the 2π phase range, it is likely that the true maxima and minima are missed. The missing of extrema tends to make both R_{12}^{+} and R_{12}^{-} smaller than their true values. The introduction of the symmetric expression partially cancels this kind of error.

From Eqs. (6) and (8) we may also obtain an identity,

$$(R_{12}^{+})^2 + (R_{12}^{-})^2 = 16. \tag{10}$$

This identity holds under ideal conditions. Noise or other forms of error can cause a deviation from it. This identity aids in the implementation of an error-correction algorithm that will be developed in Section 4.

As mentioned above, we have limited the phase shift for this calibration algorithm to between 0 and π. For precision phase calibration, this is a natural choice since it is assumed that the phase is advanced in relatively small steps. The typical goal of calibration is to correct small deviations of the phase shift from the desired phase shift. However, we will see that to calibrate a phase shifter over a large range of phase delays, the phase wrapping problem must be addressed. In Section 5 we will describe the experimental calibration of a PZT. This discussion will include a technique for unwrapping the phase. While this experiment will demonstrate the feasibility of implementing this algorithm, the accuracy of the calibration algorithm can be examined in greater detail through the use of simulated data. In particular, in

the following section on error analysis, the sensitivity of this algorithm to noise and other forms of error can be examined.

3. ERROR ANALYSIS

The possible sources of error include such common sources as intensity noise, digitization error (for an 8-bit CCD camera, only integer intensities between 0 and 255 can result), and deviation of background intensities from uniform distribution. All these errors contribute to the error in the measured cosine phase shift. When we invert $\cos\phi$ in Eq. (9), the error is further propagated to the measured phase ϕ. In this section we will first focus on this error propagation.

Note that the $\cos\phi$ reaches a local maximum and a local minimum at values of ϕ equal to zero and π, respectively. Around these points the slope of the cosine function is nearly zero so that a small change in $\cos\phi$ corresponds to a relatively large change in ϕ. Thus, for a fixed amount of error in $\cos\phi$, the error in ϕ will depend on ϕ. In particular, close to these extrema, a small error in $\cos\phi$ results in a large error in ϕ. This can be quantified by the following analysis. Suppose we have a fixed error in the measured $\cos\phi$ of δC. This will result in an error of $\delta\phi$ for a given ϕ. Making use of a first-order Taylor expansion of $\cos\phi$ gives $-\sin\phi\delta\phi = \delta C$, or

$$\delta\phi = -\delta C/\sin\phi. \tag{11}$$

Equation (11) accurately describes the error propagation for ϕ in regions away from the extrema of $\cos\phi$. When ϕ is equal to $\pi/2$ the error has a local minima. The error described by Eq. (11) is consistent with our intuitive argument. This finding indicates that a more accurate phase-shift measurement can be made if we choose a phase shift that is roughly in the vicinity of $\pi/2$. If the measurement of a small phase shift is desired, the use of a third interferogram will allow this small phase shift to be measured at roughly the same minimum level of error. However, in order to describe this quantitatively, we must first deal with the singularities in Eq. (11).

These singularities are the result of truncating the Taylor expansion at first order. To remove them, the Taylor expansion is performed to second order, and the following refined equation is obtained:

$$\frac{\cos\phi}{2}(\delta\phi)^2 + \sin\phi\delta\phi + \delta C = 0. \tag{12}$$

From this equation we obtain

$$\delta\phi = -\tan\phi\left[1 + \left(1 - \frac{2\delta C}{\cos\phi\tan^2\phi}\right)^{1/2}\right]. \tag{13}$$

Equation (13) removes the singular behavior at the extrema. Away from these points, the term $2\delta C/(\cos\phi\tan^2\phi)$ is small, so we can apply a first-order Taylor expansion to the terms inside the square root, which again gives Eq. (11).

Now suppose we wish to measure a small phase shift, ϕ_{12}, between two interferograms, which we label 1 and 2. If we apply the above algorithm directly, the phase error is significantly larger than the minimum value (a factor of 5 larger). However, we may introduce a third interferogram, labeled 3, which has approximately a 90-deg phase shift relative to the two interferograms. We may calculate the phase shifts between 1 and 3, ϕ_{13}, and between 2 and 3, ϕ_{23}. The phase shift ϕ_{12} can then be obtained from $\phi_{12} - \phi_{23}$. In this case, the error in ϕ_{12} remains of the same order as the errors in ϕ_{13} and ϕ_{23}. We will see in Section 4 that there is an alternative to this straightforward approach. An error-correction scheme can be implemented that removes the need of a third interferogram for the measurement of small phase shifts (or phase shifts in the vicinity of π).

We have also performed numerical simulations to test the error behavior. We have analyzed the root-mean-square (RMS) error in the measured phase shift as a function of the true phase shift, ϕ. In Figs. 1(a) and 1(b), the digitization error and an additive intensity noise term [amplitude of 5% of I_m in Fig. 1(a) and 10% of I_m in Fig. 1(b)] were included in the interferograms. The most dominant feature is the increase of the error as either zero or π phase shift is approached. This increase is anticipated by Eq. (13). It also confirms that near a phase shift of 90 deg, a more accurate phase-shift measurement can be made. Note that if there is no added noise (only digitization noise and a limited spatial resolution are considered), the RMS error is nearly constant for any phase step from 1 to 180 degrees. The RMS error is less than 10^{-6} deg or 10^{-8} rad. The dashed curves are the result of the error-correction algorithm, which will be developed in Section 4.

Figure 2 demonstrates the error behavior as a function of the level of the added intensity noise. The phase shift is fixed at 15 deg, a region in which the algorithm may generate relatively large errors. The solid curve in the figure shows a roughly linear increase of error as the

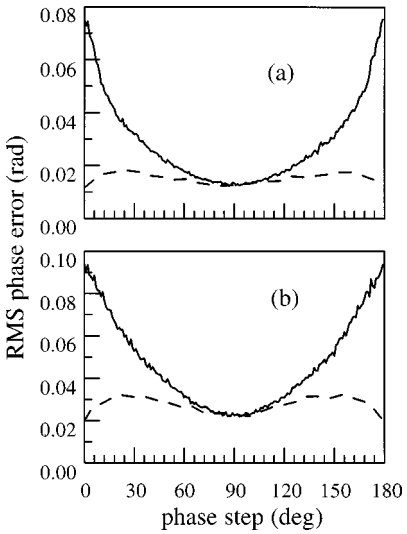

Fig. 1. RMS phase error as a function of the phase step in the presence of noise. (a) Intensity noise with an amplitude of 5% of the modulation intensity, I_m, is added to the simulated interferograms (the simulated interferograms have digitization noise). (b) Intensity noise of 10%. Solid curves, RMS error for the phase calibration at this level of noise; dashed curves, reduced error achieved by implementing the error correction scheme.

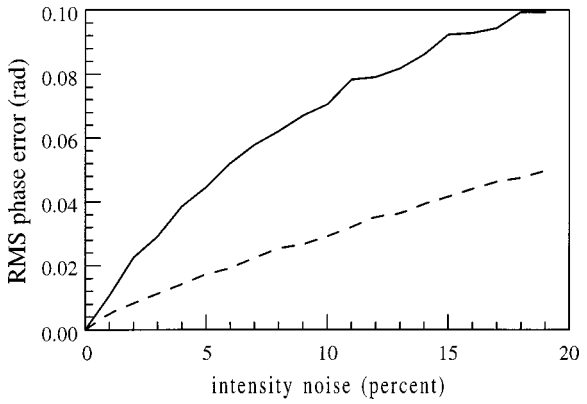

Fig. 2. RMS phase error as a function of added intensity noise. The error in the calibration of a phase step of 15 deg is measured. Solid curve, error for the calibration algorithm; dashed curve, error when the error-correction algorithm is implemented in conjunction with the calibration algorithm.

noise increases. Again, the dashed curve is the result of the error-correction algorithm discussed in the next section.

4. ERROR CORRECTION

For the phase-calibration algorithm suggested in this paper, one of the major sources of error is the error in the measured intensities of the pixels. As noted above, this can take the form of the digitization error associated with the standard CCD-array detector or result from some other noise source. However, recall the identity, Eq. (10). The presence of error in the measured intensity will cause a deviation from this identity. Thus it is possible to define a measure to gauge the error in a particular measurement:

$$\epsilon = 16 - [(R_{12}^{+})^2 + (R_{12}^{-})^2]. \quad (14)$$

In addition to quantifying the error associated with intensity noise, this measure can be used to partially correct the error. Note that in a low-noise environment that induces only small deviations from the identity, the measured values of R_{12}^{+} and R_{12}^{-} are only slightly away from their real values. We search for the closest R_{12}^{+} and R_{12}^{-} that satisfy the identity. These corrected R_{12}^{+} and R_{12}^{-} should be very close to the real values. Thus we are seeking the corrections ΔR_{12}^{+} and ΔR_{12}^{-} such that

$$(R_{12}^{+} + \Delta R_{12}^{+})^2 + (R_{12}^{-} + \Delta R_{12}^{-})^2 = 16, \quad (15)$$

and so

$$2R_{12}^{+}\Delta R_{12}^{+} + 2R_{12}^{-}\Delta R_{12}^{-} = 16 - [(R_{12}^{+})^2 + (R_{12}^{-})^2] = \epsilon. \quad (16)$$

The shortest distances from the real values of R_{12}^{+} and R_{12}^{-} are defined by minimizing $(\Delta R_{12}^{+})^2 + (\Delta R_{12}^{-})^2$. After some straightforward algebra, we find that the corrections for R_{12}^{+} and R_{12}^{-} are

$$\Delta R_{12}^{+} = \frac{\epsilon R_{12}^{+}}{2[(R_{12}^{+})^2 + (R_{12}^{-})^2]}, \quad (17)$$

$$\Delta R_{12}^{-} = \frac{\epsilon R_{12}^{-}}{2[(R_{12}^{+})^2 + (R_{12}^{-})^2]}, \quad (18)$$

The effect of this error correction on the RMS error in the measured phase is shown as dashed curves in Figs. 1(a) and 1(b). Note that the error is significantly reduced and remains nearly constant as a function of the phase shift ϕ. With an added noise of 5%, the RMS error in the measured phase shift is less than 1 deg. For 10% added noise, this RMS error increases to a little less than 2 deg.

In Fig. 2 we also show the effect on the error-correction algorithm of increasing noise. It shows a generally linear behavior, as did the calibration algorithm without this correction. However, the rate of increase of error is smaller in this case.

5. EXPERIMENTAL IMPLEMENTATION

To perform a realistic demonstration of the phase-calibration algorithm, we generated an object beam by tilting one of the flat mirrors of a Twyman–Green interferometer. There is no strong requirement on the flatness or quality of mirrors needed to perform this phase calibration. If the primary goal is to measure the phase shift, e.g., a precision measurement of displacement, relatively inexpensive optics may be used. The tilting can be easily controlled so that a full fringe can cover the region over which the background intensities are uniform. A spatial filter provides a spatially coherent beam for input to the Twyman–Green interferometer. The beam coherence aids in producing a nearly uniform background intensity over the region of interest.

The phase shifter (a PZT) is calibrated by taking a series of interferograms as the applied voltage to the PZT is increased. Both the measurement of the voltages applied to the PZT and the image acquisition are under computer control. Also, note that the selection of the region of interest, the normalization, and the finding of the extrema can all be accomplished without user intervention. The whole experiment is performed in a highly automated manner. The selected region of interest in this test case is a portion of a horizontal line of data taken from each interferogram; a horizontal tilt was introduced into the object mirror. Examples of the raw data are shown in Fig. 3. Note that in this demonstration the input beam is not perfectly spatially uniform (here imperfections of a lens are producing a high-frequency diffraction pattern on the interferogram). This high-frequency content is removed by a smoothing procedure, and the calibration can still be made quite accurately.

One approach for deriving the calibration curve from the collected data is to obtain the phase shift between each pair of neighboring interferograms and then consecutively add the phase shifts to obtain the calibration curve. However, the error that accumulates in such a process can be relatively large. An alternative method is used to avoid this type of error. We calculate the cosine phase difference between the first interferogram and all the other interferograms. In this case, we must address the phase-wrapping problem. That is, over large phase shifts the cosine phase difference between two interfero-

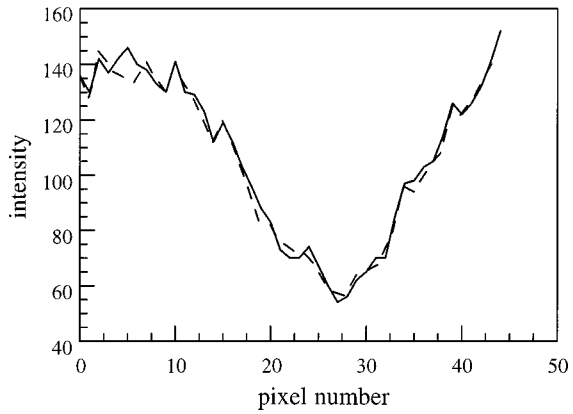

Fig. 3. Raw data from the region of interest on two interferograms. The two sets of data (solid and dashed curves) are from interferograms that have a phase separation of five cycles as determined by the phase calibration. They are nearly identical, as expected.

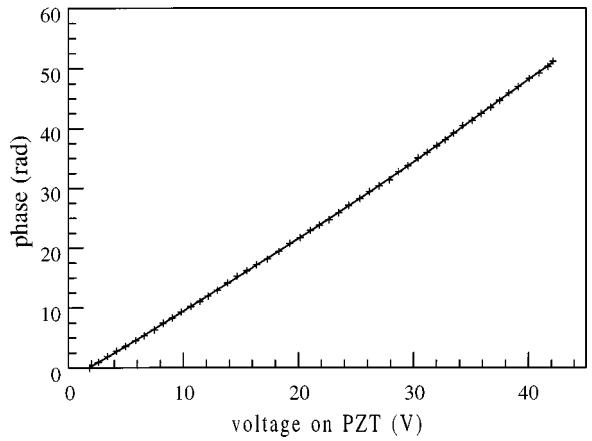

Fig. 4. Calibration curve for the phase shifter (PZT). The symbols indicate the voltages at which interferograms were recorded and the corresponding phase shifts. The solid curve is a third-order polynomial fit to these data points.

grams gives a phase that is not unique; the multiple of π that needs to be added has to be determined separately. The phase shift between each neighboring pair of interferograms can be used to resolve this wrapping problem. Knowledge of the phase shifts between consecutive interferograms is sufficient to determine the appropriate multiple π in the phase difference between the first interferogram and any other interferogram. If the phase difference between the first and the kth interferogram falls close to a multiple of π, it can lead to a relatively large error in the phase measurement (see the error analysis in Sec. 3). In that case, the second interferogram in the series is used to obtain the phase between it and the kth interferogram. Since the phase difference between the first and the second interferogram is known, the phase between the first interferogram and the kth interferogram is given by the sum of these two phases differences.

The resulting calibration curve for the PZT is shown in Fig. 4. Although the overall response of the PZT is relatively linear, a small amount of nonlinearity appears over eight cycles of phase shift. A polynomial fitting is performed, and we find that a third-order polynomial accurately describes the behavior of this PZT. This curve takes the form $\phi = -1.7534 + 0.9624V + 0.02665V^2 - 0.0015V^3$, and the data have a standard deviation of 0.1 rad from the fitted polynomial. As an indication of the quality of the calibration, we compared two interferograms that are separated by five cycles (according to the calibration). According to Wyant's technique,[4] these interferograms should be identical since they are separated by a phase equal to an integer (5) times 2π. The solid curve and the dashed curve in Fig. 3 are the raw data from these two interferograms. The two curves are nearly identical, as anticipated. This demonstration indicates that the calibration may be implemented experimentally in a straightforward manner.

6. CONCLUSION

The phase-calibration algorithm described in this paper allows an arbitrary phase step to be calibrated between two interferograms. Only these two interferograms are needed to perform this calibration. The accuracy of the method was tested numerically in the presence of digitazation noise and with added intensity noise. When only digitization noise is present, the RMS phase error is less than 10^{-6} deg. An error-correction algorithm was also developed that allows the main algorithm to be used even in the presence of large amounts of intensity noise. The method was implemented experimentally and was used to characterize a slightly nonlinear phase shifter. The accuracy of this experimental calibration was confirmed by the correlation of interferograms separated by precisely an integral multiple of 2π.

We have discussed this phase calibration algorithm primarily in terms of phase-shifting interferometry. In this case, it is likely that the optical quality of the interferometer is high. However, there is no strong requirement regarding the flatness or the quality of the optical components needed to perform this phase calibration. If the primary goal is to measure the phase shift, e.g., a precision measurement of displacement, relatively inexpensive optics may be used.

ACKNOWLEDGMENT

This work was supported by the National Science Foundation under grant PHY-9733643.

REFERENCES

1. P. K. Rastogi, *Holographic Interferometry* (Springer-Verlag, Berlin, 1994).
2. D. Malacara, M. Servin, and Zacarias Malacara, *Interferogram Analysis for Optical Testing* (Marcel Dekker Inc., New York, 1998).
3. D. W. Robinson and G. T. Reid, eds., *Interferogram Analysis* (Institute of Physics, Bristol, UK, 1993).
4. Y. Y. Cheng and J. C. Wyant, "Phase shifter calibration in phase-shifting interferometry," Appl. Opt. **24**, 3049–3052 (1985).

5. P. Carré, "Installation et utilisation du comparateur photoélectrique et interferentiel du Bureau International des Poids et Mesures," Metrologia **2**, 13–23 (1966).
6. K. Jambunathan, L. S. Wang, B. N. Dobbins, and S. P. He, "Semiautomatic phase shifting calibration using digital speckle pattern interferometry," Opt. Laser Technol. **27**, 145–151 (1995).
7. N. A. Ochoa and J. M. Huntley, "Convenient method for calibrating nonlinear phase modulators for use in phase-shifting interferometry," Opt. Eng. (Bellingham) **37**, 2501–2505 (1998).
8. Hedser van Brug, "Phase-step calibration for phase-stepped interferometry," Appl. Opt. **38**, 3549–3555 (1999).